

Generic guide concepts for the European Spallation Source

C. Zender^{a,*}, D. Martin Rodriguez^a, P. M. Bentley^{a,b}

^aEuropean Spallation Source ESS AB, Box 176, 221 00 Lund, Sweden

^bUniversity of Uppsala, Uppsala, 751 20, Sweden

Abstract

The construction of the European Spallation Source (ESS) faces many challenges from the neutron beam transport point of view: The spallation source is specified as being driven by a 5 MW beam of protons, each with 2 GeV energy, and yet the requirements in instrument background suppression relative to measured signal vary between 10^{-6} and 10^{-8} . The energetic particles, particularly above 20 MeV, which are expected to be produced in abundance in the target, have to be filtered in order to make the beamlines safe, operational and provide good quality measurements with low background.

We present generic neutron guides of short and medium length instruments which are optimized for good performance at minimal cost. Direct line of sight to the source is avoided twice, with either the first point out of line of sight or both being inside the bunker (20 m) to minimize shielding costs. These guide geometries are regarded as a baseline to define standards for instruments to be constructed at ESS. They are used to find commonalities and develop principles and solutions for common problems. Lastly, we report the impact of employing the over-illumination concept to mitigate losses from random misalignment passively, and that over-illumination should be used sparingly in key locations to be effective. For more widespread alignment issues, a more direct, active approach is likely to be needed.

1. Introduction

Ground breaking at the ESS construction site took place in September 2014 just outside the city of Lund, Sweden. At the time of writing, three of the 22 planned public instruments have already entered the detailed design phase of the construction project, with more following every year. With such a large number of instruments designed by different partners at almost the same time, it is important to identify commonalities and find cost-effective solutions to common problems in order to avoid duplication of effort and associated cost increases. Moreover, a baseline guide concept for each instrument category is a useful tool to benchmark new ideas and guide concepts.

The design of guides for a source with the characteristics of ESS has unprecedented challenges. The first challenge is the adequate geometry for efficient neutron transport over distances as long as 150 m. So far, beamlines like the high resolution powder diffractometer HRPD [1] at ISIS with a length of 100 m count amongst the longest instruments. This challenge has been addressed extensively in several studies (e.g. [2, 3, 4, 5]) by the use of ballistic or elliptic guides which minimize reflection losses. The second challenge is to reduce the extent of beam losses due to misalignments. This problem has not been addressed as extensively as the first challenge, and needs to be evaluated. The third challenge, and by no means the least important, is

the appropriate geometry to obtain low background while maintaining high transport efficiency. Beamlines between 20 m and 50-75 m face an unprecedented challenge, due to the high proton beam intensity, which places design requirements to mitigate the spallation background risk that may contaminate the useful neutron beam. This background poses a problem not only for the measurements aspiring a high signal to noise ratio, but also affects the safety design of ESS, as well as mitigation of radiation damage for components, activation, and the amount of shielding required as a consequence along the beamline.

The requirements on neutron background are particularly stringent for SANS, reflectometry, and spectroscopy. The requirements call for a noise suppression relative to the signal of around 10^{-6} and 10^{-8} in the strongest cases — see, for example, [6]. Such backgrounds are possible to achieve at spallation sources [7], but only with careful optimisation of the whole system of optics and shielding together. In this article, for brevity we concentrate on the optical part of the problem, and only describe some of the shielding in much broader terms.

Where baseline beamline shielding designs from neighbouring beamlines overlap, a common shielding area has been defined that the ESS calls the bunker. This structure is similar to other guide bunkers at existing facilities. Taking advantage of this bunker, by losing line of sight before the beamline emerges into the guide hall is one way that individual instrument costs can be reduced. Equipment in direct view of the source is illuminated by stray

*Corresponding author

Email address: carolin.zendler@ess.se, ph: +46-721792232 (C. Zender)

hadrons¹ spanning the MeV to GeV energy range, and these produce showers of secondary particles (mostly neutrons), therefore a direct view of any such secondary source has to be avoided as well. That is to say, line of sight to the source should be avoided twice. For direct geometry spectrometers, the concept of double crystal monochromators [8] naturally fulfills this condition. All other instrument classes need alternative solutions.

The magnitude of the aforementioned challenges depend on the length of the guide to some extent. It is currently anticipated that, with longer neutron guides, it will be possible to reduce the background by taking advantage of distance, and the ESS is currently examining fast neutron albedo transport. Presently, for the long guides the technical focus is on maintaining low guide costs and minimising the transport losses from misalignment. In contrast, the problem is the opposite for the short beam-lines, because the misalignment losses are less significant and the total guide costs are lower. However, the line of sight avoidance condition is severely more restrictive, and the design of a guide with a good performance and a low background becomes more of a challenge.

In this article, after establishing a basic technical grounding, we will examine medium length neutron guides of 50 m, in section 3, including both the double line of sight requirement as well as a study of misalignment, before solutions for 20 m long instruments focussing on the line of sight condition are discussed in section 4.

2. Simulation details

2.1. Simulation program

For all simulations, the Monte-Carlo ray-tracing package VITESS [9, 10] version 3.2 is used. Guide cross-sections are rectangular and gravitational effects are included by default. The neutron source that was used in the models is the ESS TDR moderator² [11]. More recent moderator developments do not change the validity of the present work, since line of sight is avoided in the horizontal direction. An adoption to a 3 cm high flat moderator (like the so-called “butterfly” which is currently planned for ESS) can easily be done by a modification of the vertical guide shape to reoptimise the vertical plane beam extraction. The difference in the horizontal geometry that the new moderators bring are most important for bi-spectral instruments, and — since this only affects the first sections of guide traversing the monolith bulk shielding, amounting to a small perturbation overall — these are not considered here. The viewable area of the moderator surface in the horizontal plane is approximately about 7 cm (cold) and 12 cm (thermal) — these are larger than the effective areas that couple to the guide, and large compared to the

2 cm beam desired for a chopper around the 6 m position (see section 3 below), therefore only a slight adjustment of the beam extraction would be needed to adapt the 50 m instrument solution to the new moderator design. Similarly, the short instrument optimization starts altogether at 6 m from the source (see section 4 below), after a simple straight monolith insert that can be adjusted independently if need be, but is with a width of 3 cm small enough to not see any difference between a 7 cm and a 12 cm wide moderator.

Supermirror reflectivity is modelled by a generalized non-linear description [12, 10]. Non-linear guide shapes are modelled using straight mirror segments.

Optimization. The main optimization routine used here is the particle swarm optimization (PSO), as available within the VITESS package since version 3.2, which follows the time-varying acceleration coefficients method [13].

2.2. Line of sight and shielding standards

In a curved neutron guide, if the radius necessary to avoid direct line of sight is calculated such that the line is exactly closed by the supermirror planes, particles along the critical trajectory traverse an infinitesimally small volume of guide substrate. Several instruments have been built with this design only to relearn the lesson that fast neutrons travel easily through glass and are not reflected by supermirrors, and those instruments suffer from background problems as a result. Therefore, the radius R of a curved guide is calculated assuming a width w' larger than the separation of the supermirrors (w) by 5 mm. In addition, the use of metal substrate guides feeding through large collimation blocks (sometimes called “horse-collars” at other facilities) in at least three parts of the curved section is planned (cf fig. 1(b)).

This is the baseline design until a minimum path length within shielding material is defined, by detailed shielding calculations.

3. Double-ballistic neutron guides for medium length instruments (50 m)

Several neutron guides are planned to be deployed at ESS as part of “medium length” instruments, corresponding to a guide length of about 50 m-75 m. For reasons of background reduction, as well as radiation safety — which essentially translate directly into instrument performance and cost — the sample and detector position should wherever possible *not* have a direct line of sight to the moderator. This is the “first line of sight” principle.

Furthermore, to avoid illumination by secondary particles, the sample and detector position should also avoid having a direct line of sight view of any equipment that lies within line of sight of the source. This is our “twice out of line of sight” recommendation. It is further advantageous for shielding cost reduction [14] to be out of line

¹Mostly neutrons, but also some protons and pions

²VITESS moderator characteristics of the 2013_Schoenfeldt database with a 12×12 cm² moderator size

of sight once within the common shielding bunker, which is foreseen to have a radius of 20 m for short instruments, and 30 m for medium and long instruments at the time of writing.

For the purposes of this study, the guide is designed with the following objectives:

- deliver high flux on a $1 \times 1 \text{ cm}^2$ sample at 50 m from source
- avoid direct line-of-sight twice
- homogeneous beam divergence
- 2 cm wide slit for fast choppers at 6.25 m
- 4 cm wide slit for choppers somewhere around half distance

These objectives capture the typical, essential features of ESS beamlines, and we study this as a generic concept not directly related to any particular instrument.

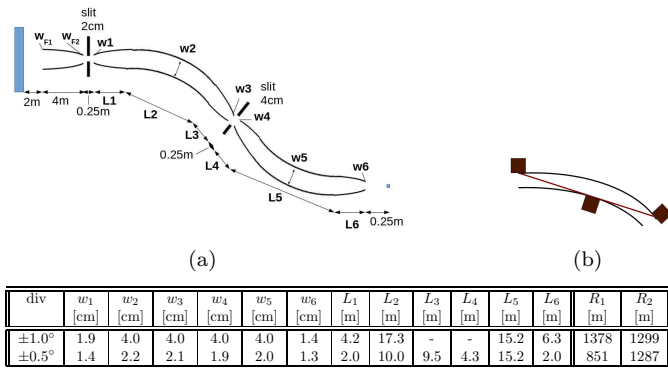


Figure 1: (a) Schematic drawing of double-ballistic curved guide and optimization results for avoiding LoS at 20m and 45m (table). (b) Schematic drawing of line-of-sight calculation and metal block placement.

Particle swarm optimization has been used to optimize the guide parameters shown in figure 1. In order to reduce the number of free parameters, the optimization started at 6.25 m with a $2 \times 2 \text{ cm}^2$ virtual source and horizontal and vertical shape were optimized separately. Only the horizontal shape is scatched in figure 1, the vertical shape either matches the ballistic shape of the horizontal plane (without the curvature) or follows a simple ellipse. The first 4 m of horizontal guide (feeder) which focus into the first, 2 cm aperture were optimized separately. Since the figure-of-merit in particle swarm optimization maximizes either the neutron throughput or the signal to noise ratio, but does not take beam quality measures like a homogeneous phase space into account, PSO was used in combination with parameter scans to obtain a high brilliance transfer as well as an approximately smooth divergence distribution.

The performance is evaluated by the shape of the divergence distribution as well as by the brilliance transfer.

The latter is calculated as the neutron intensity in a desired divergence range obtained on the sample, divided by the neutron intensity in the same divergence range and spatial area at the source. The sample area is $1 \times 1 \text{ cm}^2$. The divergence range of interest for many instruments is assumed to be $\pm 0.5^\circ$ or $\pm 1^\circ$, so we will examine both values in this study.

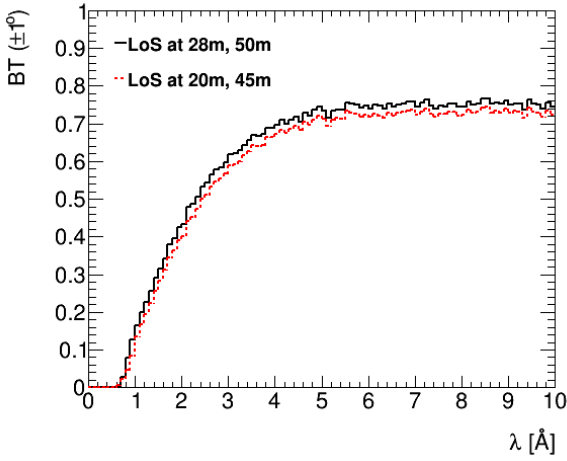
3.1. Large divergence solution ($\pm 1^\circ$)

The best performance is obtained with the parameters given in the table of figure 1: a large divergence requires a wide guide in order to minimize the number of reflections, whilst at the same time the central focusing parts can be avoided if the curved guide is of equal (or smaller) width as the central aperture, i.e. 4 cm in this case. In addition, a larger fraction of the guide can be curved if no central focusing is needed, entailing a smaller curvature with larger radius. The performance is shown in figure 2 for a square guide cross-section, comparing one option that avoids LoS twice by the end of the guide at 49.75 m with another that avoids LoS once in the common shielding bunker at 20 m and once more 5 m before the sample position. The latter option is motivated by minimising background from secondary particles produced in the shielding just before the sample position. The former entails dividing the curved part up to 20 m from the source into two channels. These additional constraints are shown to lead to only a minor loss of brilliance transfer, and the increased curvature does not add any structure to the divergence spectrum. Hence, the additional effort to avoid line of sight further away from the sample position can and should be taken when designing an ESS instrument of medium length.

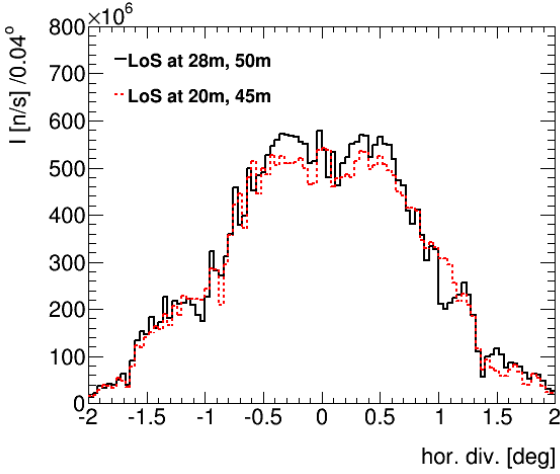
Supermirror coating. For reasons of simplicity and to limit the parameter space, the supermirror coating is fixed to a high value of $m=5$ in the optimization of the guide shape. This is of course not necessary throughout the whole surface area of the guide, in fact the transmission of the guide can be tailored towards a specific wavelength and divergence range by optimizing the coating accordingly: this is demonstrated in figure 3, which shows the BT and divergence for the guide found above that avoids LoS at 20 m and 45 m. In the example shown here, the m values are greatly reduced to optimize the coating for 2 \AA neutrons in a limited divergence range of $\pm 0.5^\circ$. No BT is lost for $\lambda \geq 2 \text{ \AA}$, with the $m=5$ coated area reduced to 1% of the guide surface and the major part of the guide coated with $m=2$ (50%) and $m=2.5$ (25%).

3.2. Small divergence solution ($\pm 0.5^\circ$)

We now explore the effect of optimising the guide shape for a smaller divergence range of $\pm 0.5^\circ$. The resulting guide parameters, delivering the best performance, are shown in the second line of the table in figure 1. The performance for a quadratic guide cross-section is shown by the black line in figure 4. Note that for this solution,



(a) Brilliance transfer



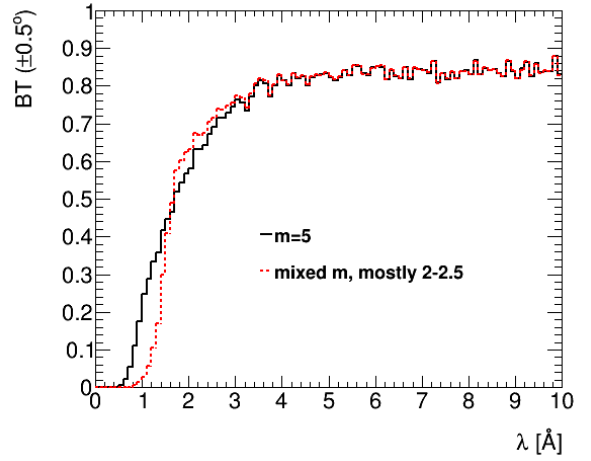
(b) Horizontal divergence

Figure 2: (a) Brilliance transfer (BT) and (b) horizontal divergence spectrum for the large divergence solution with different points of LoS avoidance as indicated in the figure legend.

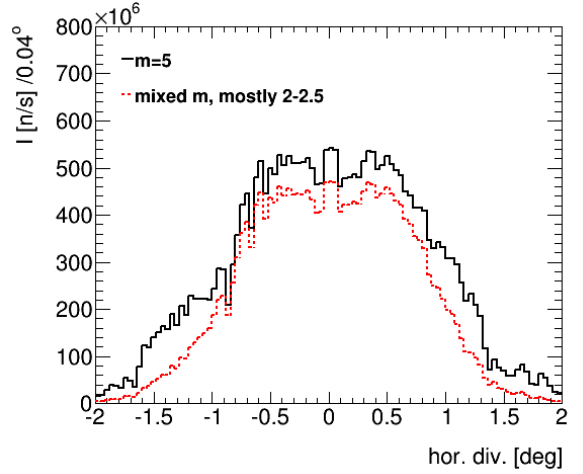
line of sight is again avoided at 20 m and 45 m from the source.

Since the 2 cm and 4 cm wide apertures at 6.25 m and 28 m from the source are motivated by choppers and have no obvious constraint in vertical dimension³, a vertically elliptic shape without any height constraints can be optimized as alternative to a symmetric guide. As expected, in that scenario the transmission efficiency increases slightly, shown by the red line in figure 4(a). However, the transmission of background neutrons would be expected to markedly increase also, and disproportionately to the thermal/cold neutrons of interest. For simplicity, we define signal neutrons as neutrons that hit the sample within the desired phase space region, whilst background here consists of neutrons that are transported to the sample plane outside the

³apart from an increase in price if the window height entails an increase of the chopper radius



(a) Brilliance transfer



(b) Horizontal divergence

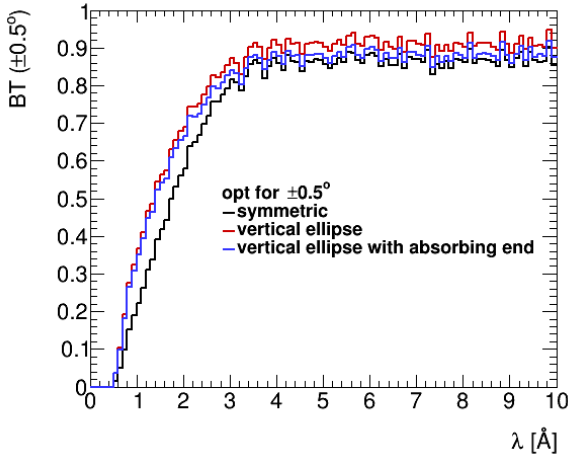
Figure 3: (a) Brilliance transfer (BT) and (b) horizontal divergence spectrum with different m -coating. Reduced coating tailored for 2 Å and $\pm 0.5^\circ$ divergence as example.

desired divergence range (type I) or outside the sample area (type II). Type I background can be seen in fig. 4(b). As shown by the blue line, this type of background can be effectively suppressed by replacing the last vertical section of the focusing guide with absorbing material (the last 2.85 m in this example) since the extra divergence the guide provides is not needed.

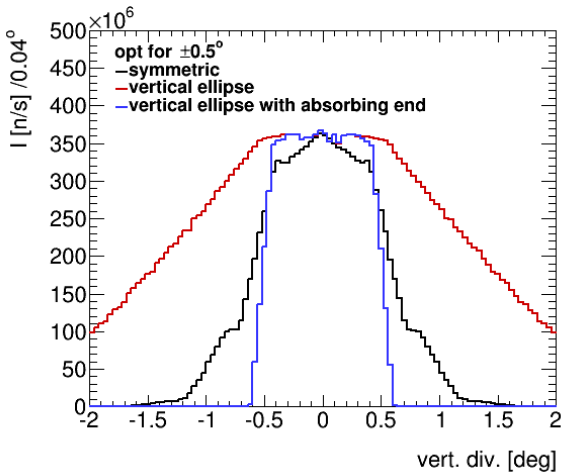
Type II background is also somewhat suppressed by this procedure, but still larger with the vertical ellipse than with a symmetric guide: the fraction of neutrons in the sample plain that hit the sample is reduced from 0.54 (symmetric guide) to 0.46 (vertical ellipse with absorbing ends). If no absorbing end section was used, this ratio would even drop to 0.34. In both of these cases one must also take care about gamma background and scattering from the surface of the absorber.

This example illustrates the importance of thinking about signal to noise ratio rather than just maximizing

the flux of neutrons on the sample.



(a) Brilliance transfer



(b) Vertical divergence

Figure 4: (a) Brilliance transfer (BT) and (b) vertical divergence spectrum for the small divergence solution with different vertical guide shapes: same height as width (black), vertical ellipse fully coated with reflecting surface (red), vertical ellipse with absorbing end sections (blue).

3.3. Random misalignment and over-illumination

Imperfections in the manufacturing and installation of neutron guides can cause a reduced performance. Especially in long beamlines, such minor effects can sum to significant impacts on brilliance transfer. A previous study measured the effect of large misalignment in one guide segment of a short miniature guide to extrapolate to the effect of small misalignment in many segments of a longer guide [15]. This approach has the advantage that the misalignment effect in the miniature guide can be experimentally verified, but the results for larger scale systems need to be validated. A simulation study of a long straight guide [16] concludes that misalignment deviations up to 0.02 mm can be tolerated for a 40 m long $150 \times 50 \text{ mm}^2$ neutron guide,

i.e. a relative misalignment of only 0.04%. An assumed absolute misalignment of $50 \mu\text{m}$ is generally used as the standard installation specification by neutron optics vendors, using laser trackers and/or theodolites. This is under laboratory conditions, and in the field we expect that thermal expansion and floor loading cause larger deviations even on relatively short timescales. Nonetheless, in the example of the 2.2 cm guide width of the small angle solution from the previous section, this $50 \mu\text{m}$ random misalignment constitutes a 0.2% geometrical uncertainty on a curved guide. We therefore explore a strategy to mitigate misalignment effects in the following section.

The concept of overilluminating subsequent guide sections to prevent misalignment effects has been successfully employed at JPARC [17], and we examine it here for the case of a double curved guide as described in the previous section. A detailed description and a possible mitigation by overillumination is given in Appendix A, here we give a summary:

1. The relative transmission of a poorly aligned guide compared to a perfectly aligned guide can be described by the function

$$T = \left(1 - \frac{2\delta}{w}\right)^N \cdot \left(1 + N \frac{f}{100} \frac{\delta/50\mu\text{m}}{w}\right)$$

where the same horizontal and vertical misalignment $\delta w = \delta h =: \delta$ is assumed for a guide of width w and height $h = w$ constructed from N independent sections. The factor $f = 0.20 \pm 0.02$ is the relative difference between gaussian and fixed misalignment per guide segment, per $50 \mu\text{m}$ misalignment and per guide width (in cm), found by simulation (see appendix Appendix A).

2. Overillumination of subsequent guide sections reduces the beamloss significantly for guides with small cross-sections, while large guides (around $10 \times 10 \text{ cm}^2$) do not benefit from this approach.
3. The beamloss caused by misalignment is not increased if the guide is curved. Losses from overillumination increase in curved guides.
4. The beamloss caused by misalignment of a ballistic guide is similar to (but slightly larger than) the beamloss in a straight guide with a guide cross-section of $(w_{\text{min}} + w_{\text{max}})/2$.
5. The beamloss caused by misalignment of a multi-channel guide is slightly higher than expected from the cross-section of a single channel, an additional loss due to the overlap of channel separating blades is visible.
6. Spatial misalignment significantly dominates angular misalignment. More specifically, the effect of an angular misalignment corresponding to a spatial misalignment per segment length, $\delta\alpha = \delta/L_{\text{segment}}$, is negligible compared to the spatial misalignment. This is also true for curved guides.

Applying these general findings to the guide of the previous section, which is double-curved in the horizontal direction with a maximum guide width of about 2 cm, and vertically an ellipse with a maximal guide height of 12 cm and a minimal one of about 9 cm (apart from the absorbing end section), it follows that an overillumination approach would not be beneficial in the vertical direction due to the large height and hence small relative misalignment of the guide, considering an alignment precision of $50 \mu\text{m}$. In contrast, overillumination is promising in the horizontal direction due to the comparably small guide width.

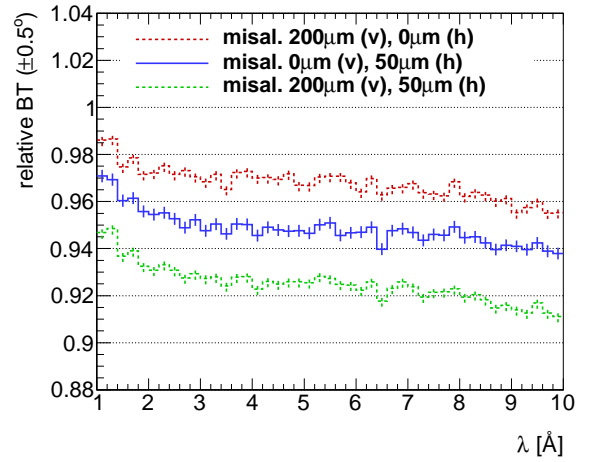
However, the largest misalignment is expected to be in the vertical direction, as the dominant process is settling of the ground under heavy shielding and construction loads. The horizontal movement is a second order effect caused by pivoting or rotations about a support point.

At ESS, an elastic vertical ground movement of 3 mm is anticipated when loading the experimental floor with shielding. In addition, a further 3 mm of creep is expected over 10 years. If we assume the possibility for re-alignment of a guide fits the facility schedule every 6 months, the latter results in additional $150 \mu\text{m}$. Therefore in the following, $200 \mu\text{m}$ are assumed vertically and $50 \mu\text{m}$ horizontally. In the simulation, guide pieces are shifted against each other by random offsets calculated from a gaussian probability distribution with these misalignment values as standard deviation, centered around $0 \mu\text{m}$. The guide is cut into 2 m long sections. The impact of misalignment is shown in figure 5(a) as the ratio of the brilliance transfer on the sample with and without misalignment. As expected from the general study, the horizontal misalignment of $50 \mu\text{m}$ causes a larger beamloss than the vertical misalignment of $200 \mu\text{m}$ due to the much smaller guide width than height. Both together lead to a brilliance loss of 5% to 9% between 1 \AA and 10 \AA . Taking the horizontally ballistic shape into account, the transmission expected from the formula above with $50 \mu\text{m}$ misalignment in the horizontal direction alone is about 96% of the transmission of the perfectly aligned guide. This is also seen in the simulation as the mean transmission ratio; when however the brilliance transfer in $\pm 0.5^\circ$ is compared instead, the loss due to misalignment is somewhat larger because in a curved guide, predominantly Garland reflected neutrons with small divergence are affected by misalignment.

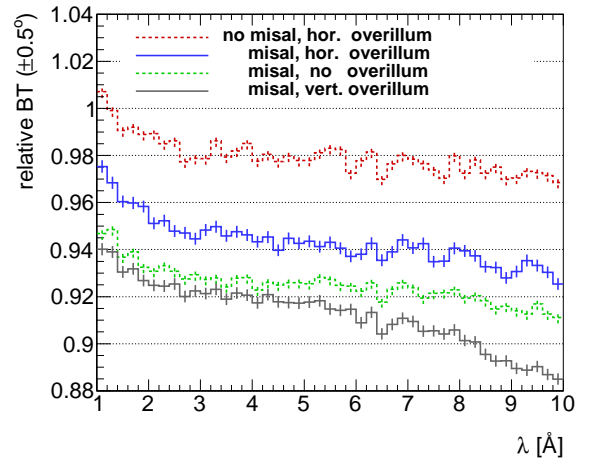
A possible mitigation by (horizontal) overillumination is shown in figure 5(b): The horizontal overillumination itself causes a beamloss between 2% and 3% depending on the wavelength. If the guide pieces are poorly aligned, the 5%-9% loss from before is reduced to 3%-7%, i.e. only a 2% gain is opposed to a 2%-3% possible loss if the guide is better aligned than expected.

The effect of a vertical overillumination is also found, as expected from the general study, to have a negative impact on transmission if it is over-used. The reason for these counter-intuitive effects is the beam extraction efficiency as the guide entrance increases in size. Consequently, we anticipate that overillumination should be used sparingly,

at one or two key locations where large floor movements might be anticipated (e.g. joins in the floor foundations).



(a) Loss from vertical (v) and horizontal (h) misalignment.



(b) Mitigation by and loss from overillumination approach.

Figure 5: Impact of misalignment and mitigation by overillumination: (a) Loss from vertical (v) and horizontal (h) misalignment. (b) Mitigation by and loss from overillumination approach.

4. Double line-of-sight with short instruments (20 m)

In this section, we examine some options for short beamlines with a sample position at 20 m distance from the source. It is of interest for all instruments to lose line of sight as close to the source as possible. This both minimises background and takes advantage of the common shielding in the bunker, to minimise instrument costs.

The options we study all lose line of sight twice, and have a monolith insert comprised of a simple, 4 m long guide of constant cross section, starting 2 m from the source. In all cases, this means that any curved or inclined guide sections are at least 6 m from the source, outside the monolith. The guide width is fixed to 3 cm. Unless stated otherwise, the supermirror coating is fixed at $m = 2$ in straight

guide parts and $m = 3$ in curved parts, again to minimise the cost of the system. Five design options are compared and evaluated at the same point, i. e., at the end of the common shielding bunker.

The options considered are as follows:

system 1 consists of a simple curved guide. This system only just satisfies the twice line of sight condition, losing 2nd line of sight right at the exit point, and having a radius of curvature of 239.26m. No instrument should build this, but we study this as an upper limit to performance with the most favourable curvature for transport efficiency.

system 2 is a single multi-channel bender, followed by a straight guide. The bender is designed such that the critical length needed to go out of line of sight is 2 m. This results in a curvature radius of 14.2 m for a 3.12 m long bender with 12 channels.

system 3 includes a double-bounce mirror in form of a kinked guide, with mirror surface and absorbing sections, such that the length of the inclined guide section is twice the length of the mirror section. Thus the inclined section starts at 6.28 m from the source and is 2×2.23 m long, the inclination angle is 0.79° and the coating of the mirror $m = 4$. Absorbing sections are designed to suppress large divergence neutrons.

system 4 uses two solid state benders of 5 cm length with 300 channels of $100 \mu\text{m}$ thickness, $m=3$ between channels, and a radius of 3.125 m. The two benders are similar in concept to the work of Krist *et al* [18]. They are separated by a straight guide of 4.5 m length. The idea of the bender design is to adjust the curvature such that it matches the critical one for the channels to avoid gaps in the transmitted divergence, which is verified in figure 6(b). The channel walls are made of silicon, simulated options for substrate materials inside the channels are vacuum (ideal maximum transmission), silicon, and carbon.

system 5 is similar to system 4, but with only 150 bender channels of $200 \mu\text{m}$ thickness coated with $m=3$, a distance between benders of 2.5 m and bender radii of 1.562 m.

Figure 6(a) gives a schematic overview over these systems and the regions in which the guide is out of line of sight twice (green), once (orange), and compared to a straight beamline (red). Curved guide sections are marked by red lines, so the very short solid benders of systems 4 and 5 appear as red stripes in an otherwise z-like geometry. For better visibility, not all bender channels are shown for system 2 and the guide is cut as it gets out of line of sight a second time, but the large offset of the beamline compared to the other options is still obvious.

Note that for all systems involving curved sections, i.e. all but system 3, the curvature and loss of line of sight

points have been calculated with an increased guide width of 3.5 cm instead of the used (simulated) 3.0 cm in order to force all neutron trajectories to pass a minimum amount of shielding material. In figure 6(a), an increased width is also drawn in systems 1 and 2 to illustrate the theoretical regions, while systems 4 and 5 illustrate the extra margin by leaving the “red” regions well before the second kink, as done in the simulations. System 3 is the only one which is both drawn and simulated without any extra margin, so an increased background can be expected there.

In case of multi-channel benders, cross-talk between channels has been modelled in the simulation.

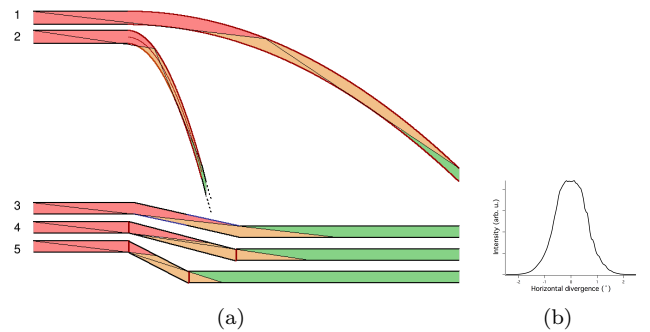


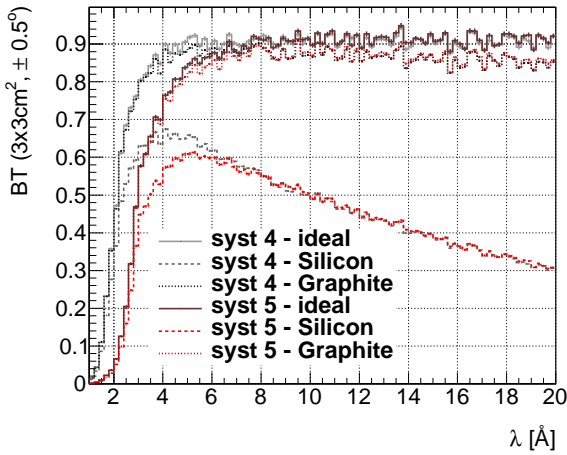
Figure 6: (a) Conceptual illustration of systems 1 - 5 (top to bottom). Red regions are within direct line of sight, orange regions have lost line of sight once, and green regions twice. Red guide walls correspond to curved sections.

(b) Horizontal divergence distribution directly after the first bender of system 4.

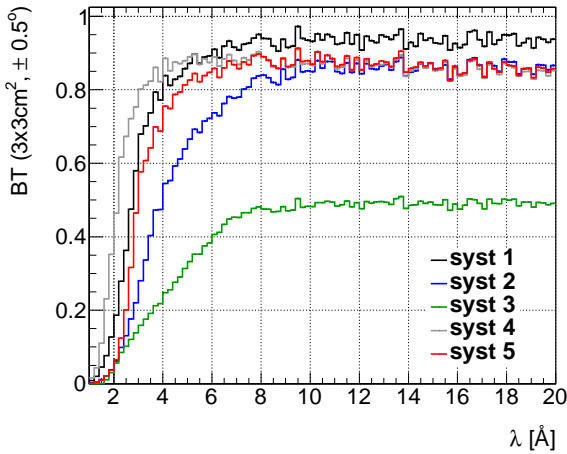
Figure 7(a) compares different options for the solid benders of systems 4 and 5: the ideal case with vacuum between the channels (solid lines) gives an excellent performance, but including the absorption of silicon (coarse dotted lines) reduces the brilliance transfer dramatically. Therefore, it is worth considering alternative materials. The third option in figure 7(a) shows the BT with solid benders made of graphite, which has a much lower absorption cross-section than silicon and therefore a very high brilliance transfer. Indeed, graphite matches the performance almost of the perfect (vacuum) case. Construction of a graphite solid state bender will depend on the possibility to manufacture graphite wafers with sheets of constant thickness and a small enough surface roughness, and it remains to be seen whether the SANS from such a system is tolerable⁴.

The brilliance transfer of all five systems, evaluated in the whole $3 \times 3 \text{ cm}^2$ guide exit region for a divergence of $\pm 0.5^\circ$, is shown in figure 7(b). The highest brilliance transfer is seen for system 1, as expected. Almost the same performance could be achieved with the graphite solid bender systems, losing only about 10% more cold neutrons and (possibly) fewer thermal neutrons than the simple curved

⁴The feasibility is currently under investigation with a prototype study.



(a)



(b)

Figure 7: (a) BT of solid benders including the absorption in vacuum, silicon or graphite. (b) Comparison of the BT of the 5 systems.

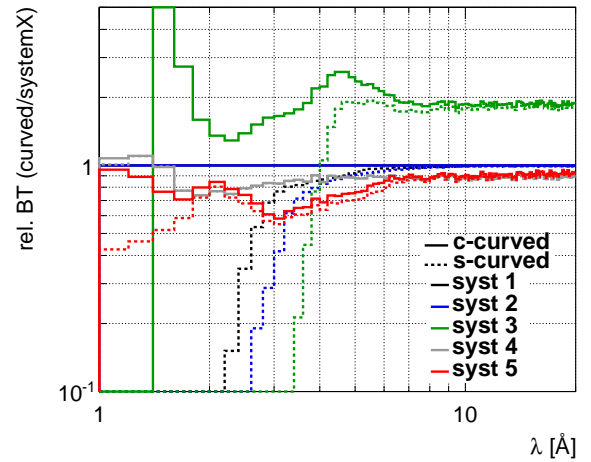
guide, even though line of sight is avoided much closer to the source. The multi-channel bender delivers equivalent performance for cold neutrons only, while losing a significant amount of thermal neutrons. The double-bounce mirror system is seen to cause unacceptably high transmission losses in the whole wavelength band.

Since all these systems lose line of sight at different distances from the source, it is instructive to compare them to simple curved neutron guides. The curved section is split into two pieces in order to compare the effect of an s-shape and c-shape curved guide. Table 1 summarises the points of line of sight closure as well as bender properties needed to avoid line of sight at the same distances from the source. As in systems 1-5, the first 4 m are just a constant guide, so the first bender extends between 6 m and the first point of line of sight, and the second bender between the first and second point of line of sight. The coating is $m = 3$ on curved surfaces and $m = 2$ otherwise. The number of channels is chosen such that the curved

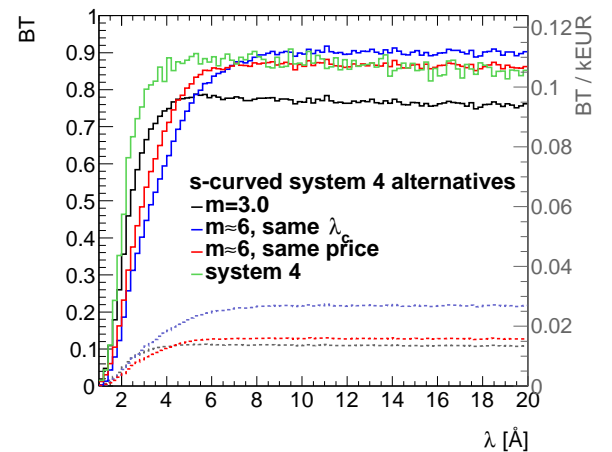
guide is as similar as possible to the original system, i.e. one channel in systems 1 and 3, and 12 channels in system 2. For comparison with the solid benders of systems 4 and 5, the number of channels is chosen such that the same λ_c is achieved.

System	1 st LoS	2 nd LoS	L_{B1}	R_{B1}	N_{B1}	L_{B2}	R_{B2}	N_{B2}	λ_c
1	11.81 m	20.00 m	5.8 m	238.0 m	1	8.2 m	239.5 m	1	3.0 Å
2	7.12 m	9.12 m	1.1 m	14.2 m	12	2.0 m	14.2 m	12	3.6 Å
3	9.74 m	14.97 m	3.7 m	114.0 m	1	5.2 m	98.0 m	1	2.0 Å
4	9.53 m	14.42 m	3.5 m	104.0 m	9	4.6 m	75.2 m	12	1.5 Å
5	7.22 m	11.49 m	1.2 m	16.5 m	14	4.3 m	65.1 m	4	3.1 Å

Table 1: 1st and 2nd point of line of sight avoidance as well as lengths ($L_{B1,2}$), radii ($R_{B1,2}$) and number of channels ($N_{B1,2}$) of corresponding benders B1 and B2.



(a)



(b)

Figure 8: (a) Relative BT of curved guides w.r.t. systems 1-5. C-curved lines of systems 1 and 2 lie on top of each other. (b) BT of system 4 alternative s-benders with different coating. Light coloured dotted lines show BT per kEUR (y-axis on right-hand side).

Figure 8(a) shows the ratio of the brilliance transfer (BT) obtained with an s- or c-curved guide to the BT of the corresponding system 1-5. Since systems 1 (black)

and 2 (blue) are c-curved options themselves, the c-ratio is just a constant line at 1, and the dotted lines directly show the transmission loss in short wavelengths of an s-bender compared to a c-bender. The s-shape reaches a BT of 90% of that of the c-shape only for wavelengths longer than 4.5 Å. This is the expected behaviour, since s-benders have the advantage of sharper short-wavelength rejection.

The kinked guide (system 3, green lines) is the only one which is a worse solution than a simple curved guide, but for $\lambda < 4$ Å it performs better than a corresponding s-bender. Note that the sharp cut-off at 1.5 Å is caused by zero statistics in the double-bounced mirror brilliance transfer, not the BT of the curved guide⁵.

The situation is slightly different for the short solid benders (systems 4 and 5), which are again evaluated assuming absorption in carbon: a simple c-shaped bender gives 90% of the brilliance transfer of those systems in most of the wavelength band (system 4) or for $\lambda > 6$ Å (system 5), and a minimum BT ratio of 75% (system 4) to 60% (system 5). Hence the solid benders perform better for thermal neutrons, while the more classical systems are a good alternative for cold neutrons without the necessity of further R&D to find the best suitable material in terms of unwanted absorption and scattering in the bender material. Interestingly, the corresponding s-bender delivers the same BT as the c-shaped guide in case of system 4, therefore the solid and dotted line lie on top of each other in most of the wavelength band.

4.1. Cost considerations

The supermirror coating of $m = 2$ in straight and $m = 3$ in curved guide sections was chosen to keep the cost low, in case of multi-channel benders it can however be cheaper to use a higher coating with fewer channels. Figure 8(b) shows the example of system 4, the BT of which is compared to s-benders with the same λ_c and either $m = 3$ or $m = 6$. The $m = 6$ option costs only about 60% of the $m = 3$ option (considering the price of the benders alone) and gives a higher brilliance transfer for long wavelengths, due to having fewer channels. The short wavelength transmission is, however, reduced because of the lower reflectivity at λ_c . The light coloured, dotted lines show the brilliance transfer per k€ is highest for the $m = 6$ option.

In comparison, an $m = 6$ option costing about the same as the $m = 3$ version is shown to give the same brilliance transfer as $m = 3$ for long wavelengths, but the brilliance transfer decreases considerably at short wavelengths.

5. Conclusions

Generic neutron guides for ESS instruments of short and medium length were optimized for good performance at low cost under the condition that a direct line of sight

to the source is avoided twice. These guides can serve as a baseline and are used to develop concepts addressing common neutron optics challenges at ESS.

It was shown that medium length instruments can avoid line of sight once within the bunker to use the common shielding as well as once more well before the sample position to avoid background without much loss of brilliance transfer. It was further illustrated that the supermirror coating should be tailored for the wavelength and divergence in mind, to effectively save money and suppress short wavelength neutrons while retaining useful neutrons, and that the coating and guide shape should be optimized such that not only the number of useful neutrons on the sample is maximized but rather the signal over background is considered.

We have shown that transmission losses from random misalignment can to some extent be mitigated by overillumination, but only for a small guide cross-section where the relative misalignment is greatest. Otherwise, the losses caused by overillumination, through poor beam extraction efficiency from having too large a guide entrance, can cause comparable or even larger losses than the misalignment if applied between all sections. Therefore the strategy for ESS is to identify high risk positions in the guide and only apply overillumination there. This means that to achieve alignment over large distances, it is likely that ESS will need to explore further options in the near future.

For short instruments (or those with very low background tolerance), the line of sight to the source can be avoided twice within 20 m from the source. A good brilliance transfer can be achieved for 2 Å and longer wavelengths without need for high supermirror coating. Different approaches for leaving line of sight as quickly as possible are presented and show that double-curved beamlines perform much better than double-kinked, and that short solid multi-channel benders are a promising approach provided that the absorption in the bender material can be controlled. To this end, a prototype study involving carbon substrates has been started.

6. Acknowledgments

We would like to thank Swiss Neutronics, Mirrortron and S-DH for their direct and indirect input into various aspects of the ESS development work leading up to this study.

References

- [1] R. M. Ibberson, W. I. F. David, and K. S. Knight. The High Resolution Powder Diffractometer (HRPD) at ISIS: A User guide. Technical report, 1992. Rutherford Appleton Laboratory Report, RAL-92-031.
- [2] K. H. Klenø, K. Lieutenant, K. H. Andersen, and K. Lefmann. Systematic performance study of common neutron guide geometries. *Nuclear Instruments and Methods in Physics Research Section A: Accelerators, Spectrometers, Detectors and Associated Equipment*, 696(0):75 – 84, 2012. ISSN 0168-9002. doi: <http://dx.doi.org/10.1016/j.nima.2012.08.027>.

⁵Infinity is set to zero.

- [3] J. Stahn, T. Panzner, U. Filges, C. Marcelot, and P. Böni. Study on a focusing, low-background neutron delivery system. *Nuclear Instruments and Methods in Physics Research Section A: Accelerators, Spectrometers, Detectors and Associated Equipment*, 634(1, Supplement):S12 – S16, 2011. ISSN 0168-9002. doi: <http://dx.doi.org/10.1016/j.nima.2010.06.221>. Proceedings of the International Workshop on Neutron Optics {NOP2010}.
- [4] M. Bertelsen, H. Jacobsen, U. Bengaard Hansen, H. Hoffmann Carlsen, and K. Lefmann. Exploring performance of neutron guide systems using pinhole beam extraction. *Nuclear Instruments and Methods in Physics Research Section A: Accelerators, Spectrometers, Detectors and Associated Equipment*, 729(0):387 – 398, 2013. ISSN 0168-9002. doi: <http://dx.doi.org/10.1016/j.nima.2013.07.062>.
- [5] C. Zendler, D. Nekrassov, and K. Lieutenant. An improved elliptic guide concept for a homogeneous neutron beam without direct line of sight. *Nuclear Instruments and Methods in Physics Research Section A: Accelerators, Spectrometers, Detectors and Associated Equipment*, 746(0):39 – 46, 2014. ISSN 0168-9002.
- [6] I. Ioffe, D. Lott, S. Mattauch, F. Cousin, A. Menelle, J. Dailant, L. Bottyan, and H. Wacklin. Ess instrument construction proposal heritage. Technical report, ESS AB, 2015.
- [7] J. R. P. Webster, S. Langridge, R. M. Dalglish, and T. R. Charlton. Reflectometry techniques on the second target station at isis: Methods and science. *Eur. Phys. J. Plus*, 126:111, 2011.
- [8] R. Kleb, G. E. Ostrowski, D. L. Price, and J. M. Rowe. A new "hybrid" spectrometer for inelastic thermal neutron scattering. *Nuclear Instruments and Methods in Physics Research Section A: Accelerators, Spectrometers, Detectors and Associated Equipment*, 106:221 – 230, 1973.
- [9] K. Lieutenant, G. Zsigmond, S. Manoshin, M. Fromme, H. N. Bordallo, D. Champion, J. Peters, and F. Mezei. Neutron instrument simulation and optimization using the software package VITESS. *Proc. SPIE* 5536(1):134–145, 2004.
- [10] C. Zendler, K. Lieutenant, D. Nekrassov, and M. Fromme. VITESS 3 - Virtual Instrumentation Tool for the European Spallation Source. *Journal of Physics: Conference Series*, 528(1):012036, 2014.
- [11] S. Peggs et al. European Spallation Source Technical Design Report. (ESS-2013-001), 2013. ESS-2013-001, ISBN 978-91-980173-2-8.
- [12] H. Jacobsen, K. Lieutenant, C. Zendler, and K. Lefmann. Bispectral extraction through elliptic neutron guides. *Nuclear Instruments and Methods in Physics Research Section A: Accelerators, Spectrometers, Detectors and Associated Equipment*, 717(0):69 – 76, 2013. ISSN 0168-9002. doi: <http://dx.doi.org/10.1016/j.nima.2013.03.048>.
- [13] A. Ratnaweera, S. K. Halgamuge, and H. C. Watson. Self-organizing Hierarchical Particle Swarm Optimizer with Time-varying Acceleration Coefficients. *Trans. Evol. Comp.*, 8(3):240–255, June 2004. ISSN 1089-778X. doi: 10.1109/TEVC.2004.826071.
- [14] P. M. Bentley. An initial cost-benefit analysis for instrument optics and shielding. Technical report, European Spallation Source, 2014.
- [15] Y. Kawabata, M. Suzuki, M. Sakamoto, T. Harami, H. Takahashi, and N. Onishi. Transmission efficiency of neutron guide tube with alignment errors. *Journal of Nuclear Science and Technology*, 27(5):406–415, 1990. doi: 10.1080/18811248.1990.9731202.
- [16] P. M. Allenspach, P. Boeni, and K. Lefmann. Loss mechanisms in supermirror neutron guides. *Proc. SPIE*, 4509:157–165, 2001. doi: 10.1117/12.448070.
- [17] Private communication between P. Bentley, K. Andersen, M. Arai.
- [18] Th. Krist, J. Peters, H. M. Shimizu, J. Suzuki, and T. Oku. Transmission bender for polarizing neutrons. *Physica B*, 356:197–200, 2005. doi: 10.1016/j.physb.2004.10.076.
- [19] I. Anderson. Neutron instrumentation part 2. In *F. P. Ricci international school of neutron science and instrumentation lecture notes*, 2014.

Appendix A. Random Misalignment

The impact of misalignment on guide performance is simulated for a generic 20 m long guide composed of 1 m long segments. The simulated neutron source is the 12 cm high TDR moderator, if not explicitly stated otherwise. This moderator is chosen to ensure a good illumination of the guide entry up to guide cross-sections of $10 \times 10 \text{ cm}^2$. The results are presented in the form of the relative transmission of the guide, including misalignment between guide segments, compared to the same guide geometry with no misalignment. As this is a comparative study, the absolute brilliance of the source can be ignored.

Appendix A.1. Spatial misalignment

Spatial misalignment is simulated as independent simultaneous shifts in horizontal and vertical direction. The magnitude of the shift is determined by a gaussian shaped random number with mean value 0 and standard deviation *misalignment*.

Appendix A.1.1. Straight Guides: Comparison of misalignment function with VITESS simulations

The transmission T' of a constant guide with misalignment, compared to the transmission T_0 of the same guide without misalignment, can be described by the following function [19]:

$$T = T'/T_0 = \left(1 - \frac{\delta w}{w} - \frac{\delta h}{h}\right)^N \quad (\text{A.1})$$

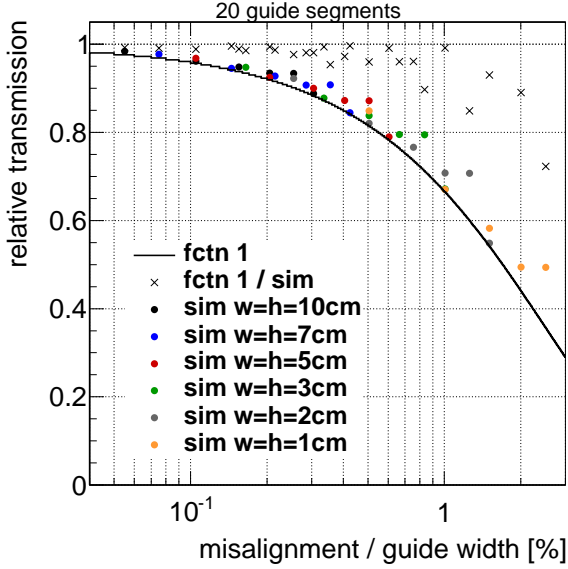
where N is the number of guide pieces, w and h are guide width and height and δw and δh the horizontal and vertical misalignment. In the following, $\delta w = \delta h = \delta$.

Figure 9(a) shows the transmission for a 20 m long guide with different cross-sections built out of 1 m long segments. Since the transmission loss depends only on the amount of misalignment relative to the guide width, the relative transmission is shown as a function of percental misalignment. The transmission predicted by function (1) is within 10% of the simulation for less than 1% of misalignment in a 20 piece guide, but systematically below the simulated transmission. The discrepancy increases with the amount of misalignment and with the guide length, as seen in figure 9(b). Hence function A.1 is only an adequate estimate of the maximum loss expected for short guides made from a small number of segments.

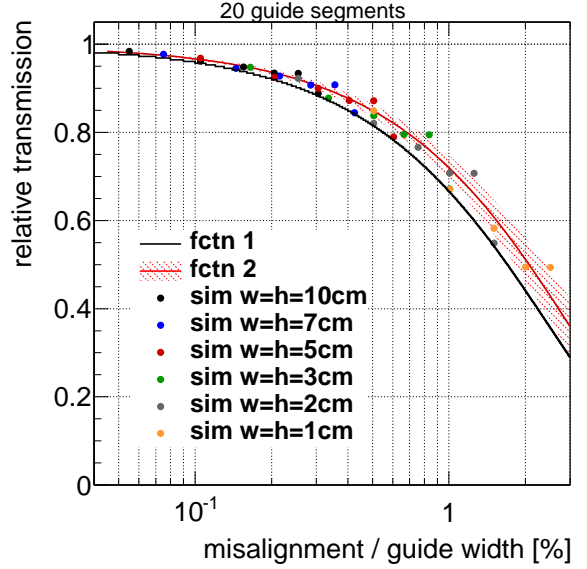
For long neutron guides made from many segments, the function systematically overestimates beam losses due to neglect of the gaussian nature of the spatial uncertainty caused by the misalignment: 68% of the joints will be better aligned than the assumed value.

Equation A.1 can be extended to reflect this effect:

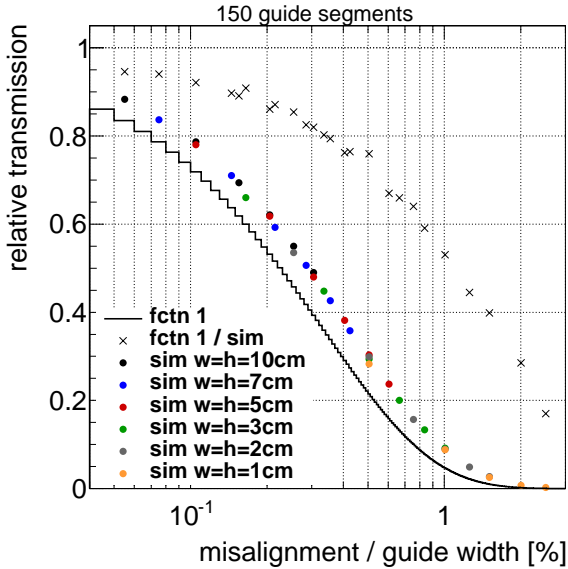
$$T = \left(1 - \frac{\delta w}{w} - \frac{\delta h}{h}\right)^N \cdot \left(1 + \frac{N}{w} \frac{f}{100} \frac{\delta}{50 \mu\text{m}}\right) \quad (\text{A.2})$$



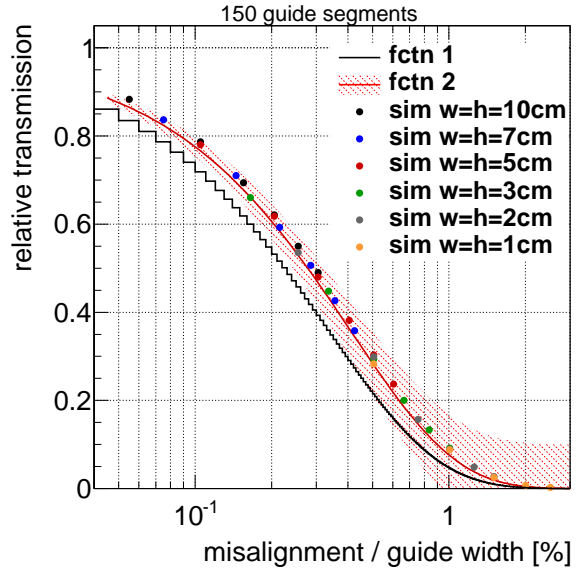
(a) 20 m guide



(a) 20 m guide, fct 2



(b) 150 m guide



(b) 150 m guide, fct 2

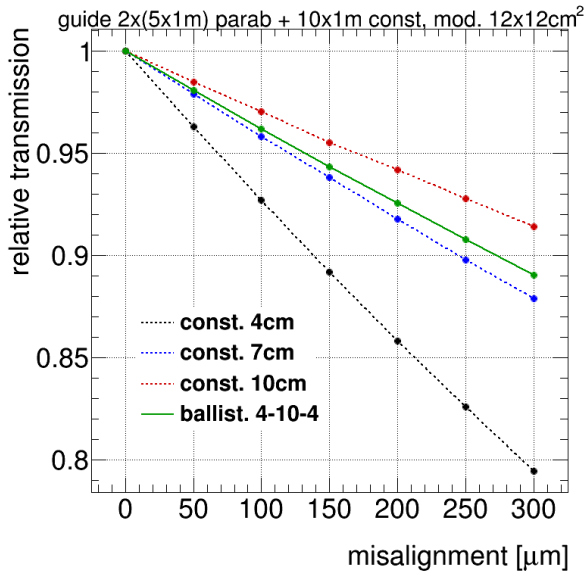
Figure A.9: Relative transmission of a (a) 20 m and a (b) 150 m guide with misalignment compared to the transmission calculated with function A.1 (solid lines), showing that the simple model applies to short guides but does not accurately predict the behaviour of long ESS guides so well. Round markers are the simulation results, and crossed markers are the ratio, with colours representing different guide dimensions as shown in the legend.

Figure A.10: Relative transmission of a (a) 20 m and a (b) 150 m guide with misalignment compared to the transmission calculated with the adjusted function A.2, showing that the improved model accurately accounts for the expected misalignments over long guides at the ESS.

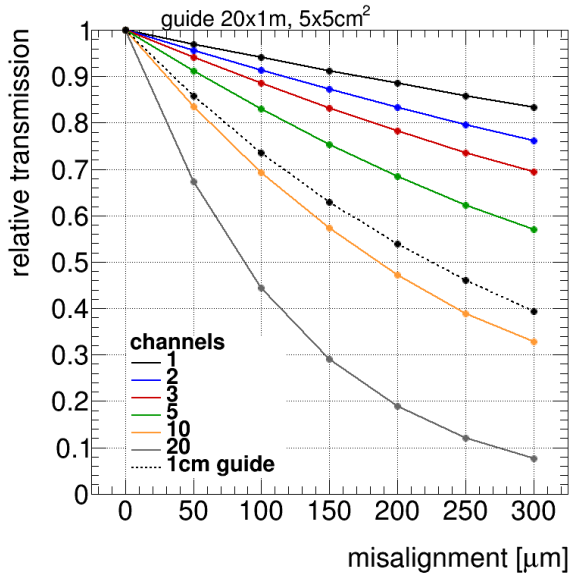
where $f = 0.20 \pm 0.02$ is the percent difference between gaussian and fixed misalignment per guide segment, per $50 \mu\text{m}$ misalignment and per guide width (in cm), extracted from 20 simulations with different random numbers for a 20 m long $3 \times 3 \text{ cm}^2$ guide and a gaussian fit to the resulting distribution of f -values. This new function is also shown in figure A.10, with a 10% error band (assuming the uncertainty of f to be the dominant one). It fits the simulated data much better than function A.1.

Appendix A.1.2. Transmission loss from misalignment in curved guides

The 20 m long guide from the previous paragraph is now curved by 19 kinks at the joints of the 1 m long guide segments, with curvature radii between 1600 m and 160 m. No difference in beamloss is observed, even for a large curvature with small R . Note, however, that in a real guide, a stronger curvature would require shorter guide segments, potentially increasing the beamlosses at the joints.



(a) Ballistic guide.



(b) Multi-channel straight guide.

Figure A.11: Relative transmission as a function of misalignment for a 20 m long guide consisting of 20 pieces. Random misalignment is modelled at each joint for $50 \mu\text{m}$, and scaled to larger misalignment. Solid lines are guides for the eye. (a) Ballistic guides of given widths, as stated in legend. (b) Multi-channel straight guides with different numbers of channels, as stated in legend, with a 1 cm square guide as a reference (dashed line).

Appendix A.1.3. Transmission loss from misalignment in ballistic guides

Figure 11(a) shows the guide loss with a ballistic guide which contains two parabolic 5 m long (de)focusing sections with equal width and height between 4 cm and 10 cm, as well as a central 10 m long 10 cm wide constant guide. The segment length is again 1 m (i.e. the parabolic shape is somewhat crude). For comparison, the beamloss of con-

stant guides with width and height equal to the maximum, minimum and medium height are displayed again. As one might expect, a ballistic guide shows losses slightly exceeding those of a medium dimensioned guide with constant cross section.

Appendix A.1.4. Transmission loss from misalignment in multi-channel neutron guides

In case of a multi-channel bender, the effect of misalignment on the transmission can be expected to be comparable to the one of a guide with a cross-section equal to one channel, plus an additional loss due to the mis-match of the channel-separating blades. For a fixed substrate thickness of 0.5 mm^6 , the relative transmission for a $5 \times 5 \text{ cm}^2$ guide with several channels is shown in figure 11(b). The guide is not curved in this example (even though a multi-channel neutron guide is usually used in combination with curvature) but, since the primary loss mechanism is the mismatch at the entrance planes, the losses as shown here should be representative.

For comparison, a 1 cm guide is shown again (dotted line): the 5-channel guide (green solid line) shows a slightly higher beamloss from misalignment than could be expected purely from its channel dimensions of $1 \times 5 \text{ cm}^2$, which would place it halfway between the $1 \times 1 \text{ cm}^2$ (black dotted) and the $5 \times 5 \text{ cm}^2$ (black solid) lines. The additional beamloss due to blade overlaps increases with the amount of misalignment.

Appendix A.2. Angular misalignment

In this calculation, we consider the impact that angular misalignment has on the transmission, angular misalignment that arises from errors in spatial positioning from the previous sections, i.e. δ , by $\delta\alpha = \frac{\delta}{L_{\text{piece}}}$. As in the previous section, the total guide length is 20 m and the guide section length is 1 m. Rotations about all three possible axes are considered in the simulation of a $3 \times 3 \text{ cm}^2$ curved guide with radius 1600 m or 160 m. The observed beamloss is negligible compared to the loss caused by a corresponding spatial misalignment ($< 2\%$ for $300 \mu\text{m}$ misalignment).

Appendix A.3. Overillumination

Overillumination is applied by expanding the dimensions of a guide upstream of a gap or location of strong expected misalignment. This removes any gaps in the phase space. This was modelled by expanding the guide section by $2 \times$ the misalignment parameter.

The result of these geometrical changes is a guide entrance that is now slightly larger than the exit. This can create issues at the beam extraction, one must take care with the acceptance of the guide entrance increasing. Clearly, the dimensions required for the neutron source can increase, and insufficient phase space at the guide entrance

⁶motivated by consultation of a possible vendor

can offset any gains in transmission efficiency. Moreover, if overillumination is applied in the horizontal plane, it can affect the radius of curvature needed to block line of sight to the source.

Omitting these adjustments here, and leaving the source size fixed to be the same as the guide exit size (a fair evaluation bearing in mind the ESS “butterfly” moderators are compact in the vertical dimension) the effect of applying overillumination in order to prevent a decreased transmission due to misalignment is investigated by simply increasing the guide cross-section backwards for each section. By so doing, we can examine if such a passive alignment strategy can be applied across the whole system. Figure A.12 shows the gain that overillumination provides in the case where misalignment is present (round markers) and where the guide has no misalignment (crossed markers).

The beamloss can be largely reduced by overillumination for small guide cross-sections (orange and green markers), while the mitigation effect gets smaller with increasing guide width, such that for example a 10 cm wide guide (black markers) made of 20 pieces loses more transmission by the overillumination approach if the guide is better aligned than expected, than it would preserve in case of misalignment. The losses here are caused by the aforementioned finite source size.

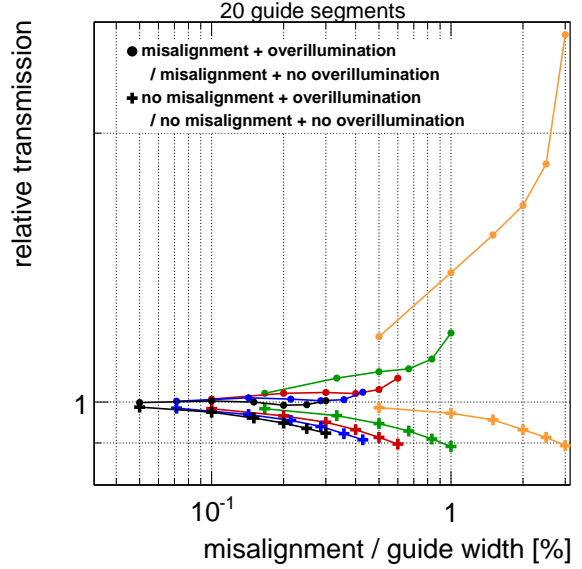
With an increasing number of guide segments, naturally both effects increase: for large guide cross-sections, the loss caused by the overillumination itself can become larger than the prevented misalignment loss even when the guide segments are as poorly aligned as expected. Applying the overillumination approach is hence not constructive in such cases. Guides with small cross-section, on the other hand, can gain even more from overillumination, so a detailed risk benefit assessment for the expected misalignment should be performed in each individual case.

For a fixed guide cross-section, overillumination becomes less effective with more guide segments. In a long guide consisting of many pieces, the overillumination approach should either be applied at a view key positions only, or designed for a smaller misalignment than expected.

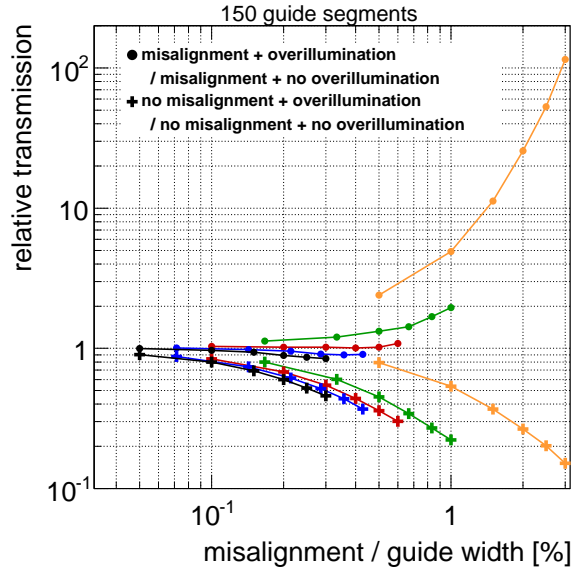
In conclusion, overillumination should certainly not be used for large numbers of elements if there is the possibility that the alignment would be better than anticipated, otherwise it creates more losses than it prevents. One should probably only use this passive method in one or two key locations where the movements are highly probable and large, such as structural joints in the floor, and particularly for guides with small cross sections.

Appendix A.3.1. Effect of overillumination in curved guides

In a curved guide, the effect of misalignment is the same as in a straight guide (cf. section Appendix A.1.2). The loss caused by overilluminating subsequent guide sections (without misalignment really being present) is slightly larger than in a straight guide, with the difference increasing with the expected misalignment. Hence the overillumination method should only be applied in curved guides



(a) 20 m guide



(b) 150 m guide

Figure A.12: Gain in transmission provided by overillumination: relative transmission as a function of percental misalignment for a (a) 20 m and a (b) 150 m long guide consisting of 1 m long segments. The source size is equal to the nominal guide width. The gain from overillumination when misalignment is present (round markers) compared to the case where misalignment is not present (crossed markers). Without misalignment, the given misalignment value merely determines the amount of misalignment anticipated in the design of the overillumination. The marker colour denotes the dimensions of the guide with the same scheme as for earlier figures (e.g. 9(a)) where black denotes: $w = h = 10$ cm; blue: 7 cm; red: 5 cm; green: 3 cm; grey: 2 cm; orange: 1 cm. Note the double-logarithmic scale.

with small cross-sections for which a significant loss from misalignment is expected otherwise.